UCRL-JC-124301

CONF-9603149--3

Impact of Environmental Conditions on the Mesoscale Characteristics of Squall-Line Systems: Toward the Development of Anvil Cirrus Parameterization for GCMs

Hung-Neng S. Chin
Michael M. Bradley

This was prepared for submittal to the
1996 Atmospheric Radiation Measurement Science Team Meeting
San Antonio, Texas
March 4-7, 1996

May 1996

Lawrence
Livermore
National
Laboratory

Impact of Environmental Conditions on the Mesoscale Characteristics of Squall-Line Systems:
Toward the Development of Anvil Cirrus Parameterization for GCMs

Hung-Neng S. Chin and Michael M. Bradley

Atmospheric Sciences Division
Lawrence Livermore National Laboratory

1. INTRODUCTION

Our earlier studies (Chin 1994; Chin et al. 1995) indicated that a strong coupling exists in the mesoscale convective systems (MCSs) between deep convection and its related anvil cloud through the interaction among dynamical, thermodynamical and radiative processes. They also showed that the tilting structure of MCSs (sub-GCM-grid feature) makes an important contribution to the water budget of anvil clouds, particularly the tropical anvil due to the jetlike wind profile. However, most earlier GCMs did not include a direct and physically consistent representation of this coupling. To this end, Randall et al. (1989) suggested a more realistic anvil parameterization by adding prognostic cloud water (or ice) variables to account for the formation of anvil clouds from cumulus detrainment. In addition to this effort, our recent studies further suggest the need to parameterize the tilting structure of MCSs in GCMs.

The objective of this work is to parameterize the large-scale effects of this tilting structure. To this end, our primary interest focuses on MCSs in an environment with substantial wind shear, such as squall-line systems, since they have longer lifetimes and wider coverage to affect the earth-atmosphere radiation budget and climate. Using varied convective available potential energy (CAPE), wind shear intensity, shear depth, and the pattern of shear profile (i.e., jetlike or non-jetlike wind profile) over a wide range of bulk Richardson number (Ri), a sensitivity study is performed in a cloud resolving model to link its resulting mesoscale ascent / descent with GCM-resolvable variables. The ultimate goal of this research is to develop an anvil cirrus parameterization (ACP), that will couple with cumulus parameterizations in GCMs to improve the cloud-radiation feedback on large-scale climate.

2. MODEL AND INITIALIZATION

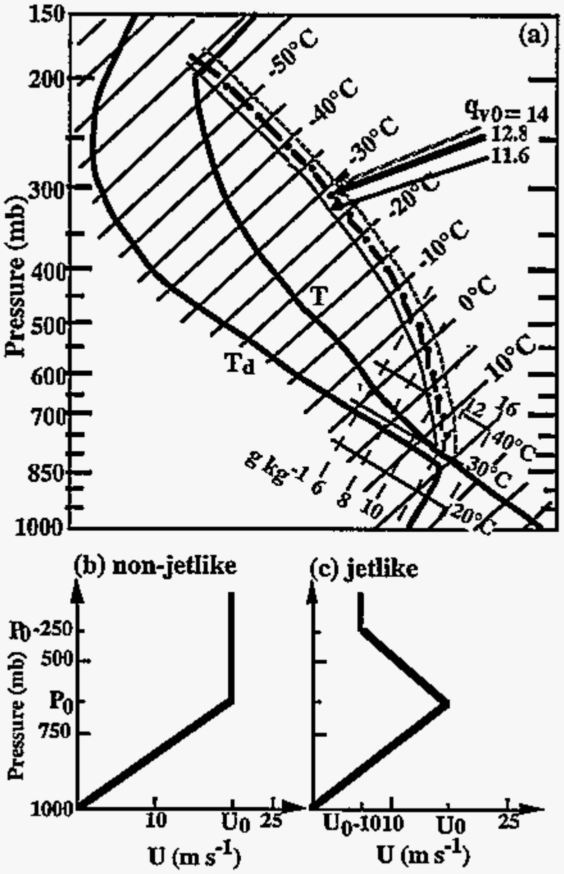

Fig. 1. The modified atmospheric composite sounding for the midlatitude broken-line squall systems. (a) temperature (T) and dewpoint temperature (T_d) profiles. moist adiabats with increasing surface mixing ratio (g kg^{-1}) of moisture represent low, medium, and high CAPE, respectively. (b) - (c) the non-jetlike and jetlike wind profiles. P_0 is set at 750 (500) mb for shallow (deep) shear layer. U_0 ranges from 10 to 25 m s^{-1}

Corresponding author address: Dr. H.-N. S. Chin, P. O. Box 808 (L-262), Livermore, CA 94551.

The model used is an extension of Chin and Ogura's (1989) two-dimensional (2-D) cloud model, which is non-hydrostatic and fully compressible. The major improvements include ice microphysics and radiation transfer schemes for long- (LW) and short-wave (SW). The modified parameterizations of ice microphysics and radiation can simulate midlatitude and tropical squall-line systems with prominent anvils and realistic mesoscale structures. The radiation schemes used can also distinguish the impacts of hydrometeor phase, size, and shape on cloud optical properties. Refer to Chin (1994) and Chin et al. (1995) for the details of model physics.

Due to the computational constraint for a large number of simulations, radiation is not considered in this sensitivity study. The prestorm conditions of this study are shown in Fig. 1, where the bulk Richardson number is chosen between 35 and 240 for multicellular convection (Weisman and Klemp 84; Fovell and Ogura 1989). The detail of these 2-D experiments is listed in Table 1, that contains a total of 36 experiments. The model is initialized by a warm, moist bubble and a horizontally homogeneous sounding.

Table 1. Design of 2-D simulations. L, M, and H stand for low (2058), medium (2704), and high (3403) CAPE (J kg^{-1}), respectively. S and D represent shallow and deep shear layer. The depth and vertical distribution of wind shear is shown in Fig. 1.

(a) Non-Jetlike Wind Profile

Experiment	1	2	3	4	5	6	7	8	9	10	11	12	13	14	15	16	17	18
CAPE	L	L	L	L	L	L	M	M	M	M	M	M	H	H	H	H	H	H
Shear Depth (B_0)	S	S	S	D	D	D	S	S	S	D	D	D	S	S	S	D	D	D
Shear Intensity (U_0)	17.5	15.0	10.0	20.0	15.0	12.5	20.0	15.0	10.0	25.0	20.0	15.0	20.0	15.0	10.0	25.0	20.0	15.0
Bulk Ri	36.9	50.2	113.	72.7	129	186.	37.1	65.8	148.	61.0	95.0	170.	46.7	83.0	187.	76.9	120.	214.

(b) Jetlike Wind Profile

Experiment	19	20	21	22	23	24	25	26	27	28	29	30	31	32	33	34	35	36
CAPE	L	L	L	L	L	L	M	M	M	M	M	M	H	H	H	H	H	H
Shear Depth (B_0)	S	S	S	D	D	D	S	S	S	D	D	D	S	S	S	D	D	D
Shear Intensity (U_0)	17.5	15.0	12.5	20.0	15.0	12.5	20.0	15.0	12.5	25.0	20.0	15.0	20.0	15.0	12.5	25.0	20.0	15.0
Bulk Ri	50.0	71.9	112.	72.9	129.	186.	48.3	64.5	147.	61.0	95.0	170.	60.7	119.	185.	76.9	120.	214.

In addition, a 3-D simulation of the GATE 4 September 1974 squall line was performed in this research (Chin and Wilhelmson 1996). The comparison of this simulation with its 2-D counterpart is used to assess the representative of 2D-based ACP into 3-D applications to GCMs.

3. RESULTS

a. 2-D sensitivity experiments

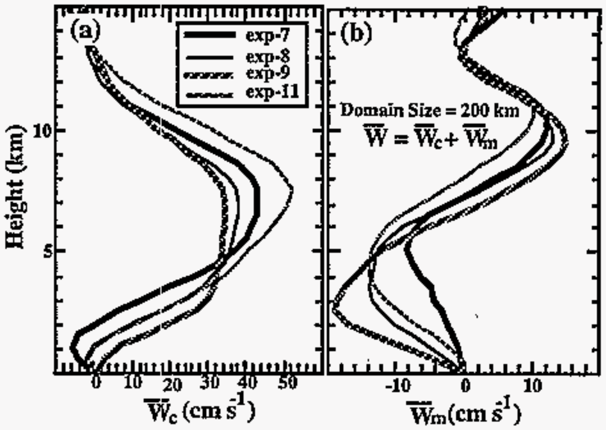

Fig. 2. Vertical profiles of domain averaged vertical velocity for experiment 7, 8 , 9, and 11. The averaging domain is selected from the leading edge to the upshear side for 200 km wide. (a) in the convective region. (b) in the stratiform region.

These sensitivity experiments are used to study the dependence of mesoscale characteristics of squall-line systems on the convective instability, wind shear intensity, shear layer depth, and the pattern of shear profile. our results indicate that under constant (medium) CAPE and constant (shallow) shear layer depth of a non-jetlike wind profile, the convective strength of the simulated storm is in positive correlation with the shear intensity, while an opposite relation is found in the stratiform region (see exp7, 8, and 9 in Fig 2). With given (medium) CAPE and shear intensity, the deeper shear layer of the non-jetlike wind profile results in stronger convective activity, while it weakens the stratiform region (see exp9 and 11 in Fig. 2). Further, under constant (medium) CAPE and constant velocity difference (U_0) of the shear layer for the non-jetlike wind profile, the deeper shear layer (i.e., weaker shear) leads to stronger convective updraft, stratiform descent, and weaker stratiform ascent (see exp7 and 11 in Fig. 2). Similar findings are also seen in each comparison for low and high CAPE, deep shear depth, and the jetlike wind profile, respectively.

The scatter diagram of stratiform ascent and Ri (Fig. 3) clearly exhibits a close correlation between maximum stratiform ascent and Ri for any given CAPE, shear depth, and shear profile. Another interesting feature of this scatter diagram is attributed to the prominent separation of two different regimes, which are related to the low and deep shear depth cases. In addition, the stratiform ascent is intensified by the jetlike shear profile and the increasing CAPE; however, these two impacts seems to be weaker than the one caused by the shear depth. All of the features aforementioned related to the stratiform ascent are also seen in its descent counterpart (not shown).

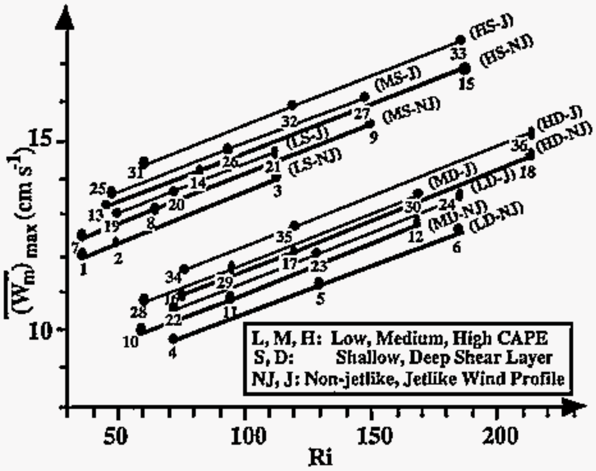

Fig. 3. Maximum stratiform ascent strength ($\overline{(W_m)}_{max}$) versus the bulk Richardson number (Ri) for varied convective available potential energy, wind shear intensity, shear depth, and shear profile pattern for multicellular storms. The numbers beside the dots represent the experiments, listed in Table 1.

In general, our results indicate that the stratiform (convective) ascent / descent is strengthened (weakened) with the increasing bulk Richardson number, except the cases involved in varied shear depths. This suggests that the shallow shear depth case should be treated differently in the ACP from its deep depth counterpart. As compared to the tropical MCS environment, the deep shear depth is a typical representative of most midlatitude cases. As a result of the secondary impact of CAPE and shear profile on the stratiform ascent / descent, the upper regime of Fig. 3 may represent the general mesoscale characteristics of tropical MCSs, and the lower one fits the midlatitude cases. However, this suggestion needs more validations for the tropical case before we can generalize the large-scale effects of the sub-GCM-grid process of concern.

b. 3-D simulation and its comparison with 2-D results

To calibrate our 2-D-based ACP into 3-D applications, we performed a 3-D simulation of the GATE 4 September 1974 squall line (Chin and Wilhelmson 1996). This 3-D simulation replicates many observed features (Houze 1977), such as the arc-shaped rainband structure and its orientation normal to the principal wind shear (Fig. 4). The comparison of 3-D and 2-D simulations in the multicellular portion of the modeled GATE storm exhibits strong similarity at the dynamical structure, except the difference at the magnitude (Fig. 5). More case studies of 3-D simulations for midlatitude MCSs are also being undertaken to establish the relationship between 3-D and 2-D simulation as the physical basis for the 3-D applications of the ACP.

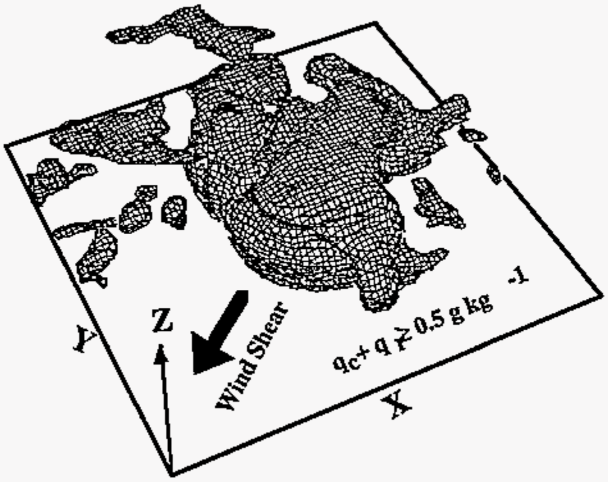

Fig. 4. 3-D depiction of the isosurface at 0.5 g kg^{-1} for the total water mixing ratio of the control run at 4 hour of simulation time. The arrow denotes the principal wind shear of environmental winds below 4 km.

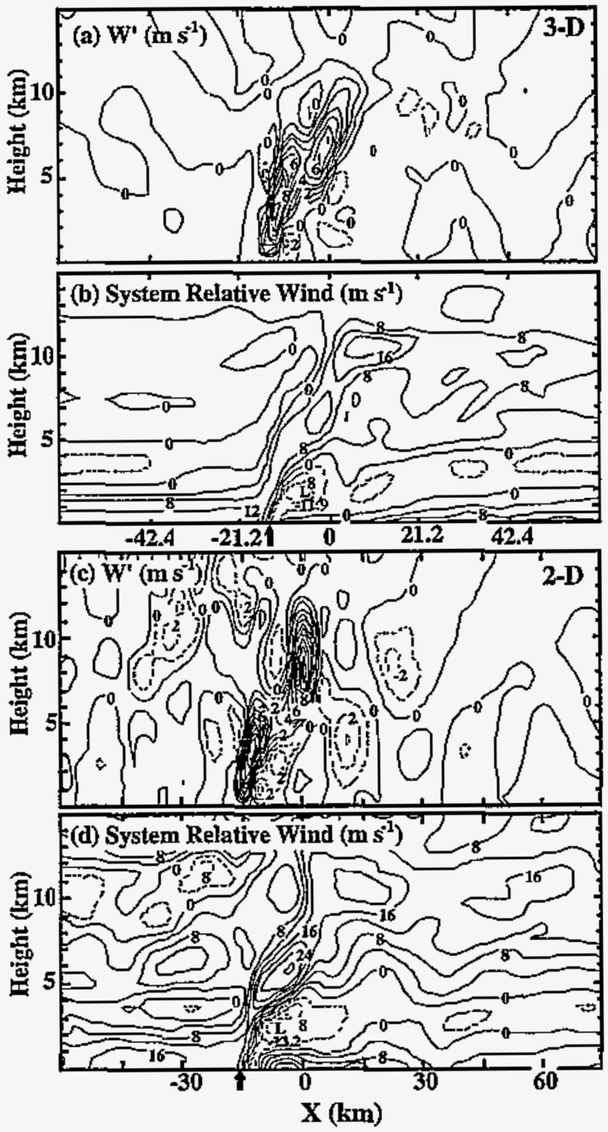

Fig. 5. Crosssections in the vertical-horizontal plane of induced vertical velocity and system-relative horizontal velocity in intervals of 1 and 4 m s^{-1} , respectively, at 4 hour of simulation time. (a) and (b) 3-D simulation. (c), (d) 2-D simulation.

4. SUMMARY AND DISCUSSION

Our results suggest that the bulk Richardson number is a valuable index to categorize the mesoscale characteristics of MCSs. Therefore, it might be feasible to parameterize the sub-GCM-grid process associated with the tilting structure of MCS.

Due to the computational constraint, we are developing our ACP, based on 2-D simulations. Nonetheless, the strong similarity of resolved mesoscale structure of MCSs between 3-D and 2-D models suggests a promising clue to calibrate the 2D-based ACP into 3-D applications to GCM.

ACKNOWLEDGMENTS. This work was supported by the Department of Energy (DOE) ARM (Atmospheric Radiation Measurement) program and conducted under the auspices of the U. S. DOE by the Lawrence Livermore National Laboratory under contract No. W-7405-ENG-48.

REFERENCES:

Chin, H.-N. S., and Y. Ogura, 1989: Supplementary modeling study of a tropical convective band. *J. Atmos. Sci.*, **46**, 1440-1447.

Chin, H.-N. S., 1994: The impact of the ice phase and radiation on a mid-latitude squall line. *J. Atmos. Sci.*, **51**, 3320-3343.

Chin, H.-N. S., Q. Fu, M. M. Bradley, and C. R. Molenkamp, 1995: Modeling of a tropical squall line in two dimensions: Sensitivity to radiation and comparison with a midlatitude case. *J. Atmos. Sci.*, **52**, 3172-3193.

Chin, H.-N. S., and R. B. Wilhelmson, 1996: Modeling of a tropical squall line in three dimensions: The arc-shaped rainband structure sustained by a supercell-like storm. *J. Atmos. Sci.*, (to be submitted).

Fovell, R. G., and Y. Ogura, 1989: Numerical simulation of a midlatitude squall line in two dimensions. *J. Atmos. Sci.*, **46**, 3144-3176.

Houze, R. A., Jr., 1977: Structure and dynamics of a tropical squall-line system. *Mon. Wea. Rev.*, **105**, 1540-1567.

Randall, O. A., Harshvardhan, D. A. Dazlich, and T. G. Corsetti, 1989: Interactions among radiation, convection, and large-scale dynamics in a general circulation model. *J. Atmos. Sci.*, **46**, 1943-1970.

Weisman, M. L., and J. B. Klemp, 1984: The dependence of numerically simulated convective storms on vertical wind shear and buoyancy. *Mon. Wea. Rev.*, **110**, 504-520.